論文 / 著書情報
Article / Book Information

論題(和文)	
Title(English)	Effect of Isolation Layer on Natural Frequency of High-Rise Base-Isolated Building
著者(和文)	黄鈺紫, 佐藤大樹
Authors(English)	HUANG Yuzi, SATO Daiki
出典 / Citation	日本建築学会関東支部研究報告集, Ⅰ, , pp. 445-448
Citation(English)	, Ⅰ, , pp. 445-448
発行日 / Pub. date	2024, 3
権利情報	一般社団法人 日本建築学会

2023年度日本建築学会
関東支部研究報告集Ⅰ
2024年3月

Effect of Isolation Layer on Natural Frequency of High-Rise Base-Isolated Building

構造ー振動　　正会員 ○ 黄 鈺紫[*1]　　正会員　佐藤大樹[*2]

High-rise base-isolated building, Observed earthquake, Natural frequency, Isolation layer, Transfer function

1. Introduction

In recent years, seismic isolation systems have found extensive application in high-rise buildings. Concurrently, there is a growing interest in analyzing structural response and parameters through structural health monitoring systems. Lee and James[1] investigated the damping effect of isolation system by using linear spring and viscous damper to model the response of superstructure. Yanagiya et al.[2] analyzed the response of non-structural members in high-rise base-isolated building by observed response data. However, research on estimating mode parameters through observed data is relatively limited.

In this paper, the recorded acceleration responses in one specific direction from three earthquakes that occurred in 2023 are utilized to estimate the natural frequency of a high-rise base-isolated building.

2. Monitoring system in a high-rise base-isolated building

This paper focuses on the J2-3 building[3] situated at the Suzukakedai campus, Tokyo Institute of Technology. Fig.1 shows a photo of J2-3 building, while Fig.2 and Fig.3 present the elevation and plan view of the J2-3 building, respectively. The J2-3 building is a 20-story high-rise structure with a height of 91.4m, comprising two interconnected buildings J2 and J3. The building is equipped with base isolation technology, with the isolation layer (MF) positioned between the 1st and 2nd stories. As shown in Fig.4, twenty-eight natural rubber bearings are installed, twenty of which are additionally equipped with U-shaped steel dampers. Furthermore, two U-shaped steel dampers and two velocity-dependent oil dampers are integrated into this layer. The 1st story of the J2-3 building is constructed with reinforced concrete and is Primarily embedded in the subsurface, assumed to exhibit rigid body characteristics. In contrast, the stories above the isolation layer are constructed with a steel framework.

Fig.5 illustrates the locations of accelerators within the J2-3 building. The arrows in the figure indicate the respective directions in which acceleration data are recorded. For instance, the accelerator denoted by a red dot on the 1st story floor of the J2 side building captures accelerations in the X, Y, and Z directions through channel numbers F000, F001, and F002, respectively. In this study, the acceleration records in X direction would be utilized for analysis.

Fig.1 Photo of J2-3 building

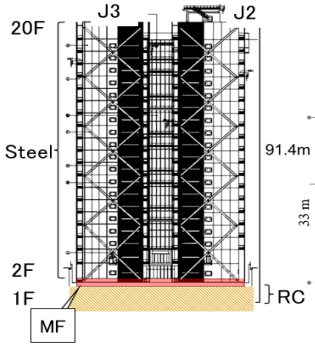

Fig.2 Elevation view of J2-3 building

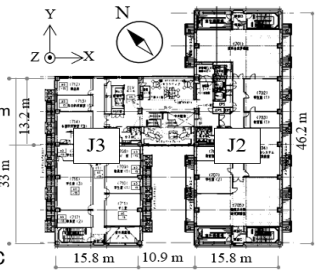

Fig.3 Plan view of J2-3 building

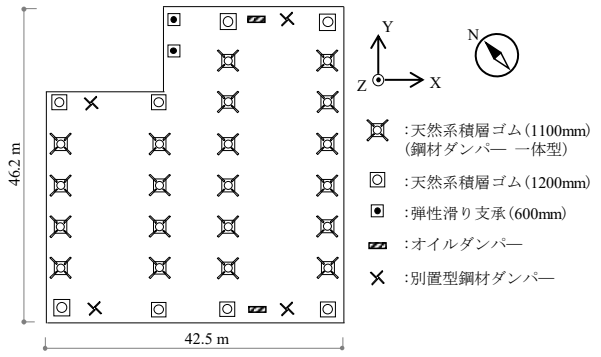

Fig.4 Layout of isolation layer

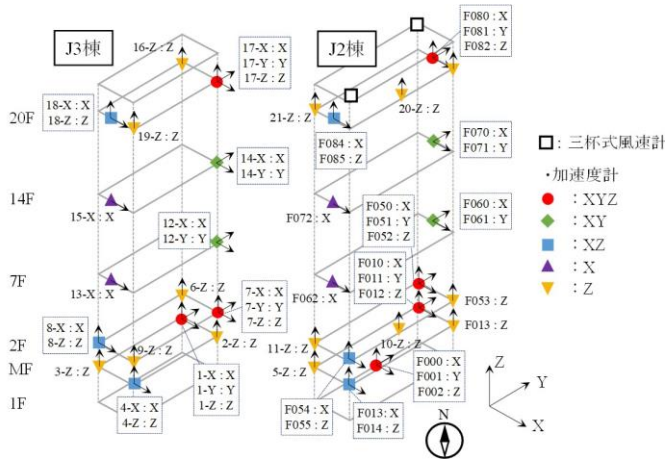

Fig.5 Locations of accelerators in J2-3 building

3. Observed earthquake data

To assess the behavior of the isolation layer during earthquakes, acceleration records obtained from accelerators on the 1st, 2nd, 20th floors of J2 side, and the 20th floor of J3 side building in X direction are analyzed. The specific channel numbers for these records are F000, F050, F080, and 17-X. As the heights of the 20th floors in both J2 and J3 side buildings are identical, and the connection between them is presumed to be rigid, the J2-3 building is treated as a unified entity during earthquakes. In this context, the acceleration of the 1st floor is considered as the ground acceleration, the 2nd floor represents the level immediately above the isolation layer, and the 20th floor is the top floor of J2-3 building.

Table.1 presents the maximum absolute acceleration values recorded on the 1st, 2nd, and 20th floors of J2, and the 20th floor of J3 side building during three observed earthquakes in 2023. Notably, the maximum absolute acceleration values of the 20th floor in J2 and J3 side building are similar, and the values also exhibit a decreasing trend from the 1st to the 20th floor in each earthquake. This trend underscores the significant influence of the isolation layer in reducing the building's response to ground motion. Moreover, Fig.6 illustrates the acceleration time history of ground motion in X direction for the three earthquakes mentioned above.

Table.1 The maximum absolute acceleration

Occurred time of earthquake	Location	Acceleration [cm/s^2] (Channel no.)	
		J2	J3
May 11, 2023 04:16	20F	3.73 (F080)	3.48 (17-X)
	2F	4.38 (F050)	-
	1F	5.18 (F000)	-
September 5, 2023 13:27	20F	2.55 (F080)	1.71 (17-X)
	2F	2.60 (F050)	-
	1F	3.42 (F000)	-
May 10, 2023 11:21	20F	1.35 (F080)	1.07 (17-X)
	2F	1.66 (F050)	-
	1F	1.94 (F000)	-

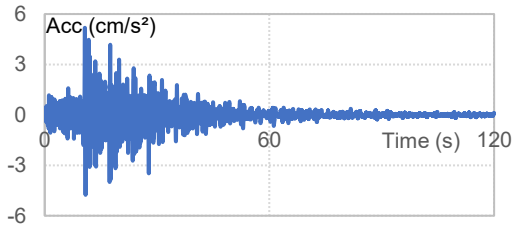

(a) May 11, 2023 04:16

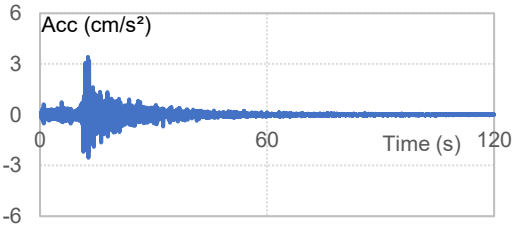

(b) September 5, 2023 13:27

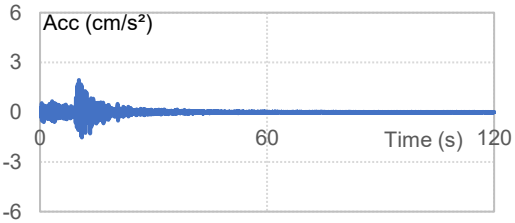

(c) May 10, 2023 11:21

Fig.6 Time history of ground acceleration in X direction

4. Data processing procedure

4.1. Analysis of transfer function

The transfer function serves as a representation of the relationship between the input and output of a system. In the realm of structural engineering, the transfer function indicates how a structure responds to various frequencies. Once the acceleration time history is obtained, the Fourier spectrum for each story can be calculated. Subsequently, the transfer function can be derived from the Fourier spectrum using the following equations.

$$|H_E(f)| = \left|\frac{F_{20}[f]}{F_1[f]}\right| \quad (1)$$

$$|H_S(f)| = \left|\frac{F_{20}[f]}{F_2[f]}\right| \quad (2)$$

In equation (1), $|H_E(f)|$ is transfer function of the entire building, f is the frequency range, $F_{20}[f]$ is the Fourier spectrum of the 20th floor within range f, and $F_1[f]$ is the Fourier spectrum of the ground within range f. In the other case, the Fourier spectrum of the 2nd, $F_2[f]$ is used as denominator in equation (2), and the transfer function of superstructure $|H_S(f)|$ would be obtained. These calculation principles are shown in Fig.7.

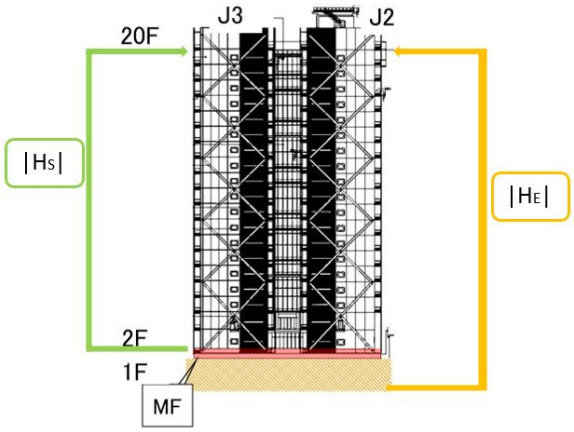

Fig.7 The calculation principle of transfer function

Fig.8 depicts the transfer functions of the entire building and the superstructure of both J2 and J3 side buildings in response to three distinct earthquakes in X direction. (a)~(c) correspond to three earthquakes, while (1)~(2) represent the cases of the entire building and superstructure, respectively. In each figure, the transfer function curves for the J2 and J3 side buildings exhibit remarkable similarity, with the same trends and peaks. Therefore, when subjected to an earthquake data input, the top floors of both J2 and J3 side buildings show identical responses and natural frequencies, which proves the rigid connection between J2 and J3 side buildings.

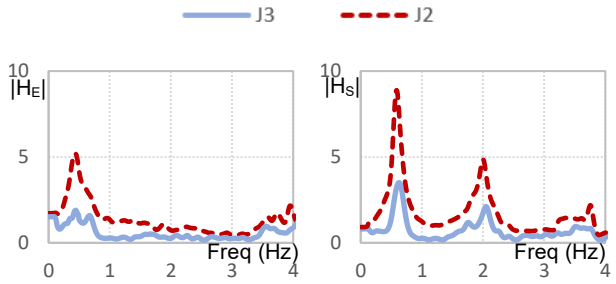

(1) Entire building (2) Superstructure

(a) May 11, 2023 04:16

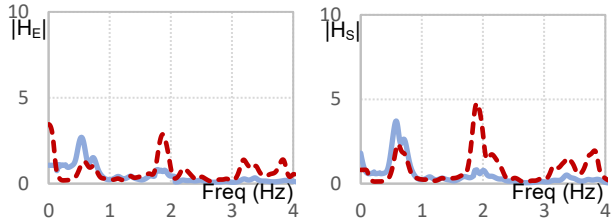

(1) Entire building (2) Superstructure

(b) September 5, 2023 13:27

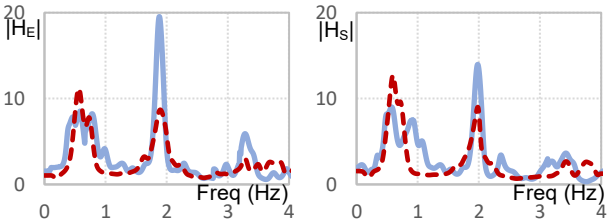

(1) Entire building (2) Superstructure

(c) May 10, 2023 11:21

Fig.8 Transfer function of J2 and J3 side buildings

4.2. Analysis of natural frequency

Drawing upon the findings detailed in Chapter 4.1, J2 and J3 side buildings are assumed as an entirety, therefore the average values of these two side buildings would be used as that of J2-3 building in the following paragraphs. Moreover, the natural frequencies corresponding to the first three modes of the J2-3 building under every condition are deduced. The abscissa values of the common first three peaks evident in the curves of each figure in Fig.8 represent the natural frequencies of the first three modes. Concurrently, the associated ordinate values signify the Fourier amplitudes at those frequencies.

Fig.9 shows the relationship between the natural frequencies of the 1st mode, f_1 (in both cases of the entire building and superstructure), and the maximum absolute ground acceleration, A_g, recorded from three earthquakes. As A_g grows larger, the difference between two curves also increases. Additionally, Table.2 shows an overview of natural frequencies of the first three modes characterizing the J2-3

building throughout three earthquakes. Herein, f_E is the natural frequency of the entire building, while f_S denotes that of the superstructure.

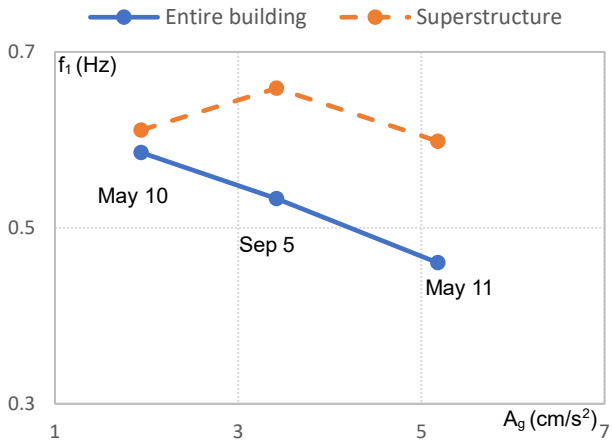

Fig.9 Relationship between the 1st mode's natural frequency and the maximum ground acceleration of J2-3 building

Table.2 Summary of the natural frequencies of J2-3 building

	1st mode	2nd mode	3rd mode
May 11, 2023 04:16			
f_E [Hz]	0.4603	1.3794	2.4597
f_S [Hz]	0.5985	2.0111	3.3106
(f_E / f_S)	0.769	0.686	0.743
September 5, 2023 13:27			
f_E [Hz]	0.5332	1.5695	3.7285
f_S [Hz]	0.6587	1.9957	3.8229
(f_E / f_S)	0.809	0.786	0.975
May 10, 2023 11:21			
f_E [Hz]	0.5857	1.8674	3.2055
f_S [Hz]	0.6112	1.9706	3.6274
(f_E / f_S)	0.958	0.948	0.884

In the context of the same mode in certain earthquakes, it is consistently observed that f_E surpasses f_S, which is indicative of the isolation layer's pronounced influence in elevating the natural frequency. Additionally, to compare the cross-examining outcomes across distinct earthquakes, combining with the findings from Fig.9, a discernible trend emerges: the stronger the earthquake, the higher the percentage increase in natural frequency attributed to the isolation layer. Notably, the maximum percentage increase in natural frequency in this study is the 2nd mode frequency during the earthquake on May 11, 2023, which reaches approximately 46%.

5. Conclusion

This paper investigates the seismic performance of the isolation layer in a high-rise base-isolated building, focusing on the J2-3 building at the Suzukakedai campus, Tokyo Institute of Technology, through the utilization of structural health monitoring systems and recorded acceleration responses in X direction from three earthquakes in 2023, the natural frequency behavior and effectiveness of the isolation layer were thoroughly examined. The analysis results are presented as following:

1) The analysis of transfer functions and natural frequencies demonstrates the rigid connection between J2 and J3 side buildings.
2) The results reveal a consistent pattern wherein the natural frequency of the entire building consistently exceeds that of the superstructure, indicating a significant effect of the isolation layer in enhancing the natural frequency.
3) The percentage increase in natural frequency due to the isolation layer is found to be influenced by the seismic intensity, with a notable maximum increase of around 46%.

In conclusion, the findings affirm the behavior of the isolation layer in enhancing the seismic performance of the high-rise base-isolated building, providing valuable insights for future structural design and earthquake-resistant strategies in high-rise structures. Further study would be conducted on system identification to analyze other parameters of high-rise base-isolated building.

Reference

[1] Lee, J.J.; James M. Kelly. The effect of damping in isolation system on the performance of base-isolated system. Journal of Rubber Research. 2019, 22, 77-89.

[2] 柳屋早延, Alex SHEGAY, 佐藤大樹, 超高層免震建物の地震時における非構造部材の応答: 最大応答加速度による分析, 日本建築学会関東支部研究報告集 1, pp.509-512, 2023.2.

[3] 大木洋司, 山下忠道, 盛川仁, 山田哲, 坂田弘安, 山中浩明, 笠井和彦, 和田章, 超高層免震建物の長期観測システム構築に関する具体的取り組み, 日本建築学会技術報告集, 第 21 号, pp.73-77, 2005.6.

*1 東京工業大学 大学環境· 社会理工学院 大学院生

*2 東京工業大学 准教授· 博士（工学）

*Graduate Student, Tokyo Institute of Technology

*Associate Prof. , FIRST, Tokyo Institute of Technology, Dr. Eng.